The Mechanism of 2,4-Dichlorophenoxyacetic Acid Neurotoxicity on Rat Brain Tissue by Using FTIR Spectroscopy

Gehan A. Raouf[1]*, Safaa Y. Qusti[2], Awatef M. Ali. [3] and Tahani H. Dakhakhni[4]

[1] Medical Biophysics Lab., King Fahd Medical Research Centre; Biochemistry Dept., King Abdulaziz University, 21551 Jeddah –KSA B.O.Box:42805, Spectroscopy Dep. Physics Div.-National Research, Cairo- Egypt.
[2,4]Biochemistry Dept., Faculty of Science, King Abdulaziz University, Jeddah –KSA
[3]Zoology Dept., Faculty of Science, Alexandria University-Egypt.
gehan_raouf@hotmail.com - jahmed@kau.edu.sa

Abstract: Previous studies demonstrated that the herbicide 2,4-dichlorophenoxyacetic acid (2,4-D), toxicity may be due to cell death by apoptosis. 2,4-D is approved to be associated with many disorders especially neurotoxicity. FTIR spectroscopy and transmission electron microscopy were used to investigate the neurotoxicity induced by LD_{50} dose of 2,4-D onto the cerebellum rat brain tissue. In response to 2,4-D stress, there is a significant increase in the intensities as well as bands area of 3463cm^{-1} , 3276cm^{-1} and 3165cm^{-1} bands; the first band corresponds to the changes in the number of lipids hydroperoxyl and to lipid hydroxyl groups formed by oxidation. There are decrease in membrane lipid polarity, increase the disorder and the looseness of lipid chain packing and a significant increase in the formation of carbonyl compounds. Moreover, protein content and secondary structure were significantly influenced upon 2,4-D intoxication. Consistent with the IR results, EM analysis revealed morphological changes in the 2,4-D treated cerebellum tissue including nuclear damage with massive condensation of chromatin, mitochondrial matrix swelling, loss of cristae and rough endoplasmic reticulum dilatation and vesiculation. Thus, 2,4-D influences membrane lipid polarity, fluidity and protein order, in addition to the morphological changes all of which can be considered as apoptosis biomarkers.
[Gehan A. Raouf, Safaa Y. Qusti, Awatef M. Ali. and Tahani H. Dakhakhni. **The Mechanism of 2,4-Dichlorophenoxyacetic Acid Neurotoxicity on Rat Brain Tissue by Using FTIR Spectroscopy** *Life Sci J* 2012;9(4):1686-1697] (ISSN:1097-8135). http://www.lifesciencesite.com. 259

Key words: Fourier transform infrared spectroscopy (FTIR), Neurotoxicity, Apoptosis, 2,4-Dichlorophenoxyacetic acid (2,4-D),Transmission Electron Microscope (TEM).

1. Introduction

Since the early 1990s, it has been argued that many chemicals used for agricultural, industrial or domestic purposes can enter the food chain, and produce a number of disorders in animals and man. (1)

2,4-dichlorophenoxyacetic acid (2,4-D) is a selective herbicide, with highest toxicity to broadleaf plants, used around houses, gardens, in agriculture and forestry.(2) 2,4-D is easily adsorbed into human from the alimentary tract and skin and excreted in the urine in nearly unchanged form.(3)

It was approved for 2,4-D to be associated with neurotoxicity,(4) hepatotoxicity,(5) immunotoxicity,(6) teratogenesis,(7) endocrine disruption,(8) and renal toxicity.(9)

It is also suggested that 2,4-D causes cell apoptosis as a result of changes in membrane potential in mitochondria and initiating of caspase-dependent reactions.(10) It is believed that the mechanism of toxicity of many compounds concerns the formation of reactive oxygen species (ROS), including superoxide anion, hydrogen peroxide, superoxide radical and hydroxyl radical.

In this study we have used FTIR spectroscopy to investigate the toxicity induced by 2,4-D onto the cerebellum rat brain tissue, looking for a double objective:

a- To monitor the neurotoxicity and the oxidative stress induced by 2,4-D intoxication by using FTIR spectroscopy and Transmission Electron Microscope (TEM) in cerebellum rat brain tissue.

b- To prove that FTIR parameters employed in this study can be used as biophysical indicators of toxin-induced cell/or membrane damage as a result of apoptosis.

2. Materials and Methods

i- Experimental Animals

The experimental work of the present study was conducted at the King Fahd Medical Research Center, Medical Biophysics Laboratory at King Abdulaziz University, Jeddah, Saudi Arabia. This study was carried out using a total number of 15 male albino Wister rats supplied by the King Fahd Medical Research Center, with a mean initial body weight of 250-350 g. The animals were grouped by randomized design and were housed individually in plastic cages in a room with a relative humidity of 70%, temperature of (24±1°C), and exposed to a light and dark cycle of 12 h duration. The first group (5 rats) is

the control and the second group (10 rats) is the 2,4-D treated group (2,4-D) that received a single oral gavage LD_{50} dose of 639mg/kg body weight of 2,4-D were then sacrificed 24hrs after 2,4-D administration. All rats received the same basic diet in pellet form Grain Silos and Flour Mills Organization, Jeddah, Saudi Arabia and water as beverage. Diet and water were supplied *ad-libitum*.

The individual animal body weight was recorded then animals were killed by decapitation and brains were rapidly removed, washed with saline and then divided into two parts in Eppendorf tubes. The first part was immediately immersed in liquid nitrogen and stored at −80 °C in a deep freeze. All samples were lyophilized prior to infrared analysis. For fixation, glutaraldehyde was added to the second part for TEM analysis until assayed.

ii- Electron microscopy

The dissected cerebellum was fixed with glutaraldehyde in 0.2 M Phosphate buffer for 5–6 hrs at 48°C. The fixed brains were cut into approximately 1mm cubes. The cubes were post fixed in 2% OsO_4 for 2 hrs at 48 °C and then dehydrated in an ethanol series. The pieces were embedded in EPON/812 taab, cut into 0.5 mm thick sections using ultra microtome (LKB Sweden) and mounted on Nickel grids (300 mm). The sections were double stained with uranyl acetate and lead citrate and then examined by TEM (Philips CM100, Netherlands) and photographed.

iii- Infrared spectroscopic measurement

The FTIR spectra from the lyophilized samples were obtained from KBr pellets according to [11]. Infrared spectra from three rats represented each group were recorded using a Shimadzu FTIR-8400s spectrophotometer with continuous nitrogen purge. For single rat, the IR spectra were obtained from different KBr disks and then coadded. Typically, 20 scans were signal-averaged for a single spectrum and at spectral resolution of 4 cm^{-1}. To minimize the difficulties arising from unavoidable shifts, each spectrum was baseline corrected, normalized as normalization produces a spectrum in which maximum value of absorbance becomes 2 and minimum value 0. Other normalization methods such as normalization to amide I band had also been tested and gave negligible changes in the results. Pellets were scanned at room temperature in the 4000–400 cm^{-1} spectral range. Background spectra, which were collected under identical conditions, were subtracted from the sample spectra automatically. After co-adding all IR spectra obtained from each group, each group is now represented by one IR spectrum, the entire spectra were normalized and baseline corrected by using IR solution software. Treating the spectra with Kubelka Munk algorithm was also performed by using the same software. Deconvolution and the best fits for decomposing the bands in the spectral region of interest were obtained by Gaussian components using Omnic software in order to increase the resolution of the overlapping bands. The parameters studied were proteins and lipids. The absorbance ratios were taken from the raw spectra.

Statistical analysis

Different absorbance ratios for specific bands were calculated. An analysis of variance (Mann-Whitney test) was conducted to confirm the results obtained from IR measurements.

3. Results

In this study, the neurotoxic effect of pesticide 2,4-D was investigated with FTIR spectroscopy by monitoring different functional groups. Representative infrared spectra of cerebellum rat brain tissue taken from cont. and 2,4-D treated groups are shown in Fig. 1a. The figure shows typical infrared spectra of biological tissues belonging to proteins, lipids carbohydrates and nucleic acids. The main absorption bands together with their proposed band assignments are given in Table 1 according to the literature. [12] [13]

Careful examination of the of the IR spectra revealed that there are no differences between the spectra of the groups under investigation apart from slight changes in the band intensities and frequencies shift.

The wide overlapping of bands in the raw spectrum results in a difficulty in band segregation and their assignment, and so using raw spectrum in the interpretation of data may not be totally conclusive as a result of noisy raw data. [14] Thus, treating the raw spectrum with Kubelka Munk algorithm, which is used here for illustrative purposes only (Fig. 1b), and/or later peak resolving may be the solution for this issue. [15]

Fig.2 shows the curve-fitting analysis, the absorption band intensities, frequencies, half band width (HBW) and area were also given in (Table 2) as the intensity and/or more accurately the area of the absorption bands are considered to be directly related to the concentration of the molecules.[16]

Detailed spectral analysis will be discussed here in three distinct frequency ranges, namely 3700-3050cm^{-1}, 3050-2800 cm^{-1} (C-H stretching region) and 1800-1500 cm^{-1} respectively.

1- Analysis of Hydroxyl and Hydroperoxyl Bands

The spectroscopic measurement of peroxides in brain tissue samples is usually used to determine the oxidative stress levels. Peroxide determinations can

be carried out by many different ways such as the νOH band of hydroperoxides located in the 3500-3000 cm^{-1} region.[17] This procedure is reliable for dried samples as in case of the lyophilized brain samples enrolled in this study.

In the raw spectra, the region 3600-3050 cm^{-1}, which is characterized for O-H and N-H stretching vibrations of lipids and proteins, shows important changes in the intensity and the shape of this broad band.

The band at 3300 cm^{-1} corresponding to the amide A stretching mode can be associated with N-H stretching and intermolecular O-H molecules. Probable IR bands due to N-H vibrations from amide A can be hidden by the more intense O-H stretching vibrations upon oxidation.[18] The intensity of the OH stretching bands (3600 cm^{-1} - 3100 cm^{-1}) reveals the degree of lipid oxidation and the amount of hydroxyl-containing lipid like cholesterol.[19]

By using a curve fit algorithm, the peaks for OH from lipids resolved into two major and two minor bands (Fig. 2a). The band intensity at 3467 cm^{-1} is perceptive to the changes in the number of lipids hydroperoxyl groups formed by oxidation.[20] The other band intensities are sensitive to lipid hydroxyl groups formed by oxidation, while the amide B band centered around 3066cm^{-1} is an indicator for the protein content in the brain tissue.[19] In response to 2,4-D stress, there is a significant increase in the intensities as well as bands area of 3463cm^{-1} , 3276 cm^{-1} and 3165cm^{-1} bands while a marked reduction in the area of amide B (around 3068cm^{-1}) band is observed in comparison to the cont. group. In addition, the amide B band centered at 3068.84cm^{-1} was shifted to lower frequency (3066.37) upon 2,4-D treatment (Table 2).

These results are also confirmed with the observed decrease in specific protein ratios. Amide A/Amide B, Amide I /νas(CH_2) ratios were calculated and are used here as a spectroscopic quantitative measurements of protein content in rat brain tissue (Table 3). Upon 2,4-D intoxication, the observed decrease were [from 1.975± 0.04, 1.385±0.1 to 1.855± 0.07, 1.349± 0.1] in Amide A/Amide B ratio and Amide I /νas(CH_2) ratios respectively.

2- The region 3050-2800 cm^{-1}: Symmetric and asymmetric stretching of methyl (CH_3) and methylene (CH_2) functional groups

Other strong bands in the spectra of these brain tissues are found to be centered in the 3000-2800 cm^{-1} region, which corresponds mainly to the CH stretching vibrations of lipids hydrocarbon chains.[21]

The characteristic spectral behavior of these bands upon lipid oxidation can be considered as a different alternative method for peroxide determinations and could be a measurement of the CH stretching bands, which because of oxidation can result in disordering of hydrocarbon lipid chains and subsequent increase of the corresponding half-band widths and/or band area.[22]

The spectral behavior of the lipid νCH bands in this region reflects 2,4-D oxidation. The decomposing of this region (Table 2) revealed that, primary oxidation products in the cerebellum treated brain tissue induce significant changes in the physical state of the lipid acyl chains. These changes are presented in the form of band shapes, frequency shifts, half widths, peak heights , and integrated intensity of the decomposed vibrational bands.[21] Compared with the untreated brain sample, the stretching bands of CH_2 groups at 2921 and 2866cm^{-1} in 2,4-D stressed samples show significant broadening (HBW) towards higher frequency (Table 2).

By contrast, the intensity, HBW and the area of the 2866cm^{-1} band relative to that of the 2921cm^{-1} band has decreased from control to 2,4-D treated sample. To explore the lipid chain polarity and order due to 2,4-D toxicity, certain lipid intensity ratios were calculated. νas(CH_2) / νs(CH_3) ratio is used here as a measurement of environmental polarity as it increases with the polarity of lipid chains environment and νs(CH_2) / νs(CH_3) ratio which is correlated with the looseness of lipid chains packing (Table 3). Also, the slight observed band shift towards higher frequency in the stretching CH_2 band centered at 2922.769cm^{-1} in control to 2922.899cm^{-1} in 2,4-D stressed samples indicates a change in membrane fluidity. Thus, the higher the frequency the higher the membrane fluidity.[23]

3-The region 1800-1500 cm^{-1}

In response to 2,4-D treatment, the intensity value of the amide I centered at ~1654cm^{-1} which is commonly associated with the infrared stretching vibrations of C=O in proteins is dramatically decreased (Fig. 1b). This decrease was consistent with the earlier observed decrease in the amide B band area and HBW around 3066cm^{-1} (Table 3).

For further investigation of this region, deconvolution and the best curve-fit for amide I band contour of the tested groups were carried (Fig. 2b). The data presented in (Table 4) summarize the calculated positions, the corresponding secondary structure of proteins and the fractional percentage areas of the amide I component bands from cont. and 2,4-D treated groups.

It is observed from (Table 4), that the area percentage of α-helix secondary structure is decreased from 21.81% to 18.34%, while the total area

percentage of β-sheet structure increased from 60.05 to 66.87 due to 2,4-D toxicity.

4- Analysis of Carbonyl Bands

The peak shoulder present at 1735 cm^{-1} can be contributed to the ester C=O stretching of phospholipids [24], not present in DNA and proteins. The esterified band C=O at 1735 cm^{-1} is strongly associated with lipids so that any shift in the frequency of this band can be directly correlated with alterations in the state of intramolecular hydrogen bonding of the interfacial region of the phospholipids structure with water and/or some functional groups of other molecules.[25] An increase in this band intensity in response to 2,4-D toxicity was observed (Table 2).

To examine the weight of formation of carbonyl compounds against lipase action or lipid degradation during lipid oxidation, the ν(C=O) /Amide II ratio was calculated (Table 3). There is a significant increase in this ratio due to 2,4-D intoxication. The decomposing of the band around 1735cm^{-1} shows two peaks at ~1720cm^{-1} and ~1741cm^{-1} (Fig. 2b). The first was decreased in area from 31.87 to 30.968, while an increase in the area around 1741cm^{-1} from 28.001 to 32.901 after treatment was detected. Both bands were shifted towards higher frequency in response to 2,4-D toxicity (Table 2).

Electron microscopy

To provide further insight to the nature of the neuronal cell death caused by 2,4-D and in order to know if the biochemical changes observed after 2,4-D administration were strong enough to leave an impact on the morphology from control and treated group, we examined the cerebellum tissue for morphological changes by transmission electron microscopy.

At the electron microscopic level of cerebellum sections in cont. group most neurons were found to possess relatively normal cell membranes, round euchromatic nucleus (Fig. 3a) surrounded by contact nuclear envelope, small ovoid or rod shape mitochondria, short parallel rays of rough endoplasmic reticulum with attached ribosomes and secretary granules in normal nucleus – cytoplasmic ratio (Fig. 3b). It is very remarkable to mentioned that mitotic division was noticed (Fig. 3c) as cytokinasis- stage which still have the cytoplasmic connection (Fig. 3d). In 2,4-D treated group, brain cells contain numerous cells undergoing apoptosis and the majority of dying cells are neuron cells. In addition to the most well-known classical apoptosis, which is characterized by early nuclear collapse and massive condensation of chromatin with polymorph-mitochondria that have dense matrices Binukumar *et al.*[26] (Fig. 3e), shows late nuclear damage type, which involves massive vacuolization of the cytoplasm with delayed collapse of the nucleus, the cytoplasm being consumed by expansion of the lysosomal system, mitochondrial matrix swelling and loss of mitochondrial cristae with dilatation and vesiculation of rough endoplasmic reticulum (Fig. 3f) the same results were obtained by Kaur *et al.*[27] and Sharma *et al.* [28]

4. Discussion

The mechanism of toxicity of many compounds concerns the formation of reactive oxygen species (ROS), including superoxide anion, hydroperoxide, superoxide radical and hydroxyl radical. These compounds are capable of reacting with proteins, nucleic acids, lipids and/ or molecules that lead to changes in their structure and finally to cell damage or cell death.[29]

Oxidative stress has been proved to occur in response to different doses of pesticides as 2,4-D [5] leading to neurochemical changes.[22] Therefore, the spectroscopic measurement of peroxides in brain tissue samples is of interest to determine levels of the oxidative stress.

Table.1: General assignment of the FTIR spectra of brain tissue in the 3600-445cm^{-1} spectral rang

Wave number (cm^{-1})	Band assignments
3301	Amide A: mainly **ν**(N–H) of proteins
3072	Amide B: **ν**(N–H) of proteins
3014	Olefinic **ν**(HC=CH): lipids
2956	**vas**(CH_3): mainly lipids
2921	**vas**(CH_2): mainly lipids
2873	**vs**(CH_3): mainly protein
2852	**vs**(CH_2): mainly lipids
1735	Carbonyl **ν**(C=O): lipids
1654	Amide I: **ν**(C=O) of proteins
1544	Amide II: **δ**(N–H) and **ν**(C–N) of proteins
1462	**δ**(CH_2) stretch: mainly lipids
1396	**vs**(COO^-): fatty acids and amino acids
1236	**vas** (PO^{-2}): mainly phospholipids
1082	**vs**(PO^{-2}): mainly nucleic acids; **ν**(HO–C–H): carbohydrates
1000-455	Fingerprinting region: mainly nucleic acids

(**ν**: stretching vibrations, **δ**: bending vibrations, **s**: symmetric, **as**: asymmetric).

Table 2: Wave numbers, intensities, HBWs and areas of different IR spectral regions.

Groups	Wave number (cm-1)	Intensity	HBW	Area
	The region 3600-3050 cm^{-1} (Hydroxyl and Hydroperoxyl			
Cont.	3463.486	3.746	257.786	1027.984
	3276.96	3.437	199.243	728.926
	3165.49	0.752	83.283	66.637
	3068.848	1.583	115.399	194.422
2,4-D	3467.536	4.026	273.577	1172.24
	3272.619	3.367	209.578	751.24
	3157.246	0.806	90.298	77.46
	3066.365	1.586	100.46	169.587
	The region 3050-2800 cm^{-1} (CH_3) and (CH_2)			
Cont.	2962.205	1.506	26.507	42.483
	2922.769	4.047	43.021	185.349
	2858.683	2.174	53.432	123.671
2,4-D	2962.741	1.486	26.948	42.624
	2922.849	3.962	44.627	188.229
	2858.58	2.175	52.553	121.646
	The region 1800-1500 cm^{-1} (carbonyl bands)			
Cont.	1741.302	1.437	18.307	28.001
	1720.75	1.152	25.993	31.87
2,4-D	1741.52	1.6517	18.7128	32.901
	1722.045	1.2551	23.179	30.968

Table 3: IR intensity absorbance ratios with standard deviation as spectroscopic quantitative measurements of protein content and membrane lipid environment in rat brain tissue.

Ratios/Groups	Cont.	2,4-D
Amide A/B	1.9753 ± 0.04	1.8548 ± 0.07*
Amide I /vas(CH_2)lipids	1.3848 ± 0.1	1.3498 ± 0.1
vs(CH_2)lipids/ vs(CH_3)lipids	1.2509 ± 0.04	1.1870 ± 0.06*
vas(CH_2)lipids/ vs(CH_3)Lipids	1.9083 ± 0.05	1.8148 ± 0.07*
ν(C=O)lipids/Amide II	0.4595 ± 0.03	0.5103 ± 0.02*

Values are means±S.D. For three rats each group. Significance is at **$p < 0.01$**. * means highly significant.

Table 4. Curve fitting analysis expressed as a function of areas of main protein secondary structures and their band assignments for control and 2,4-D intoxicated brain tissues.

Wave number (cm^{-1})	Band assignment	Cont. area % percentage	2,4-D area % percentage
1612-1621	**β-turns**	**13.13**	**13.12**
1634-1639 1641	**Parallel unordered structure**	**18.15**	**14.77**
1650-1657	**α-helix**	**21.81**	**18.34**
1666-1669	**β-turns**	**31.66**	**28.68**
1672-1677	**Parallel β-sheets**	**1.39**	**7.96**
1681-1687	**β-sheets**	**3.22**	**7.71**
1694-1698	**Anti-parallel β-sheets**	**10.65**	**9.4**

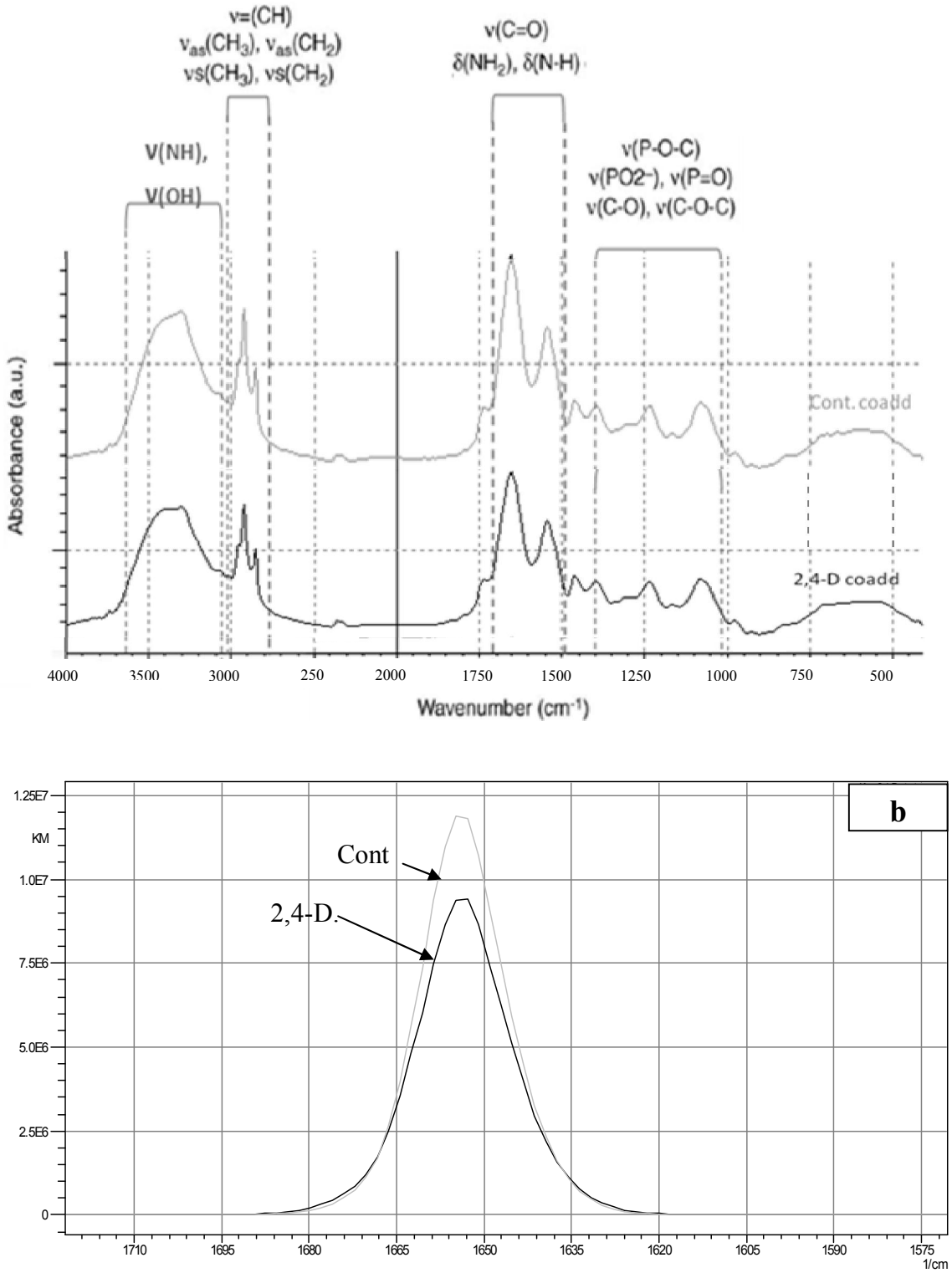

Fig. 1: **(a)** FTIR spectra of cont. and 2,4-D treated rat cerebellum brain tissue. Characteristic functional groups at specific wave numbers are indicated in the figure.
(b) Kubelkamunk spectra of brain tissue of cont. and 2,4-D treated group in the 1800-1500cm^{-1} IR spectral region.

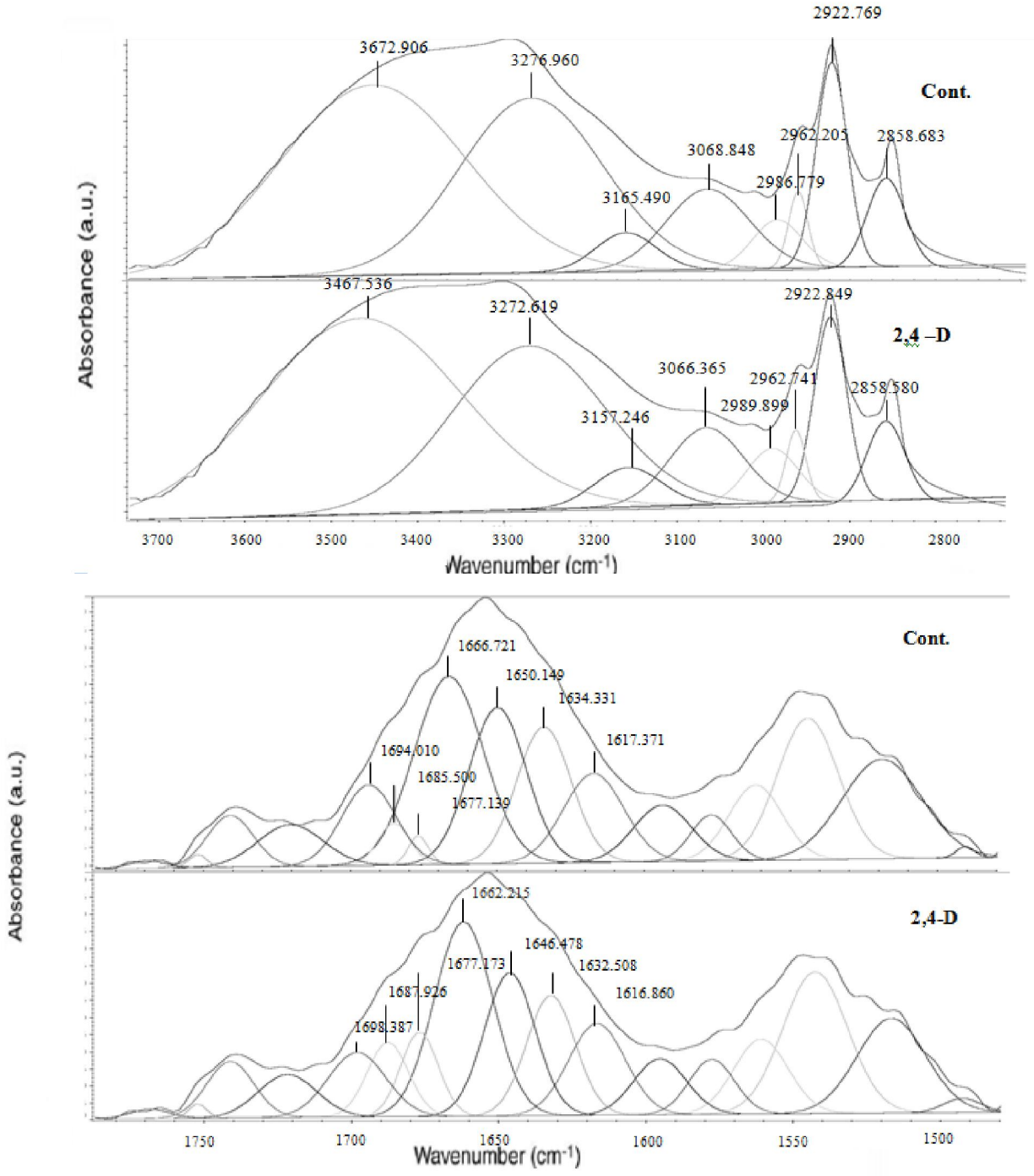

Fig. 2: **(a)** Curve fitting of brain tissues of cont. and 2,4-D group in the FTIR 3700-2700cm^{-1} spectral range (O-H, N-H stretching and CH vibrations).
(b) Deconvolution and Curve fitting for the amide I amide band in brain tissue for control and 2,4-D groups.

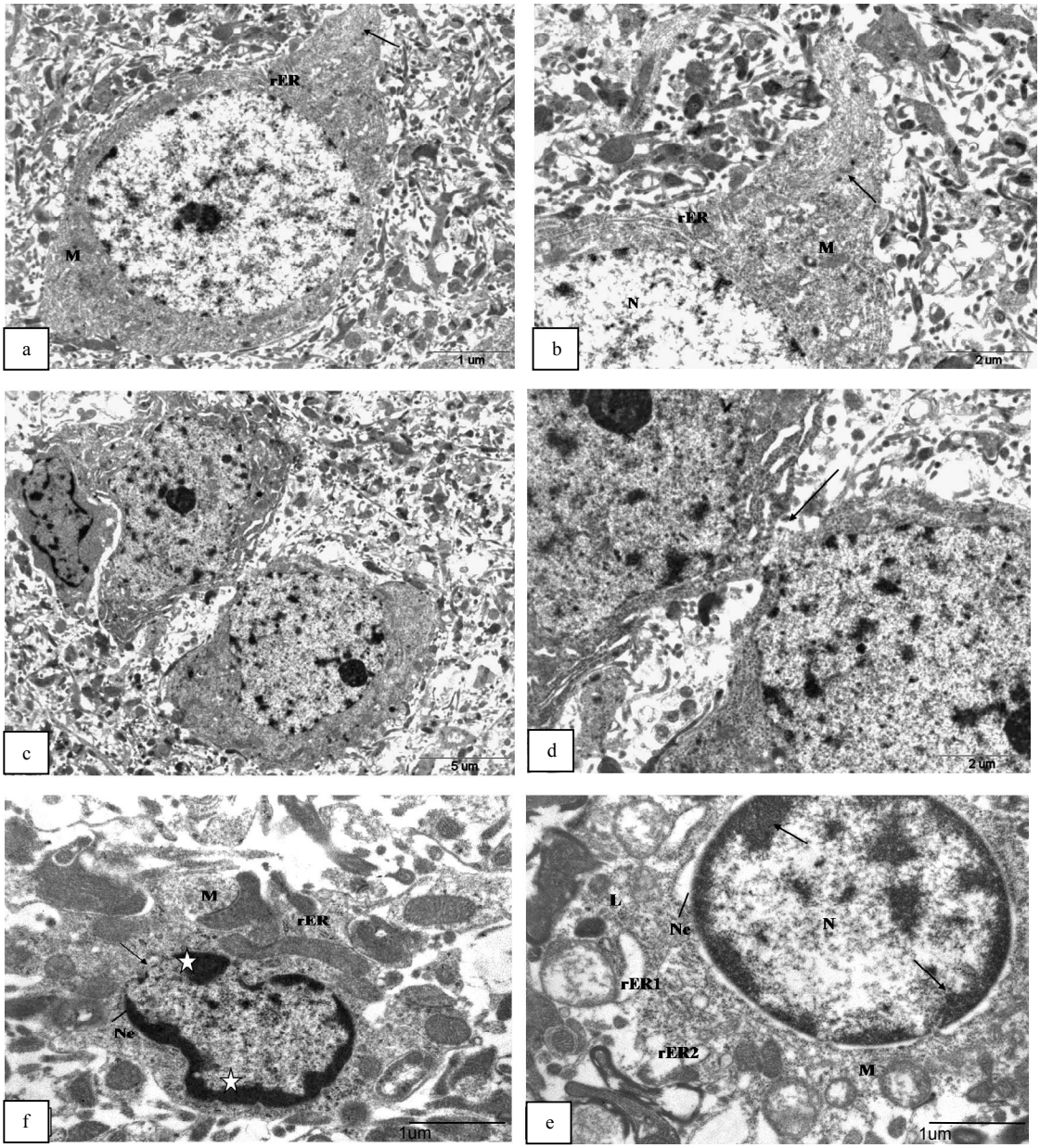

Figure 3: Transmission electron micrograph of the control cerebellum of rat brain sacrificed after 24h showing

(a) : Normal appearance of neuron with tree-like dendritic (arrow) have nucleus (N) ,small ovoid mitochondria (M), rough endoplasmic reticulum (rER) in normal nucleus –cytoplasmic ratio (x4600).

(b) Enlarged part of the pervious figure showing: Normal nucleus (N) surrounded by contact nuclear envelope ,small ovoid mitochondria (M), long parallel rays of rough endoplasmic reticulum (rER) with attached ribosomes and secretory granules (arrow) (x7900).

(c) Control cerebellum of rat brain sacrificed after 24h showing mitotic division in cytokinasis stage (x3400).

(d) Enlarged part of the pervious figure showing: Normal neuron cell in cytokinasis stage still have the cytoplasmic connection (arrow) (x7900).

(e) Cerebellum of rat brain sacrificed 24h after2,4-D treatment showing: apoptotic cell with shrinkage neuron nucleus (N) have chromatin condensation (stars), wide pores (arrows) and contact nuclear envelope (Ne) . Polymorph-mitochondria (M) with dense matrix and rough endoplasmic reticulum (rER)(x13500).

(f) Another apoptotic cell from same group with round neuron nucleus (N) have chromatin condensation (arrows) and surrounded by diluted nuclear envelope (Ne). Not, swollen mitochondria (M) with loss of cristae, dilated rough endoplasmic reticulum (rER1) or vesiculated (rER2) with detached ribosomes and lysosome (x13500). (Lead citrate & uranayl acetate).

The significant increase in the intensity as well as band area of 3463cm^{-1} , 3276 cm^{-1} and 3165cm^{-1} bands upon 2,4-D intoxication could be attributed to an increase in lipid oxidation as the intensity of the OH stretching bands (3600 cm^{-1} - 3100 cm^{-1}) reflects the degree of lipid oxidation and the amount of hydroxyl-containing lipid such as cholesterol.[19] Hydrophylic OH groups added to the hydrophobic region of lipid hydrocarbon chains with oxidation would be expected to disrupt Van der Waal's interactions between adjacent hydrocarbon chains, thus disordering the membrane. [19] Compared with the untreated brain sample, the stretching bands of CH_2 groups at 2921 cm^{-1} and 2866cm^{-1} in 2,4-D stressed samples show significant broadening (HBW) towards higher frequency. This means that, upon oxidation, the lipid chains are more disordered and there is conversion of lipid hydrocarbon chain *trans* rotomers to more gauche rotomers, which results in the mentioned band broadening and frequency shift (Table 2). These results agree with Borchman *et al.* [19] who stated lower frequencies indicated fewer *gauche* rotomers and higher hydrocarbon chain order. The intensity, HBW and the area of the 2866cm^{-1} band relative to that of the 2921cm^{-1} band has decreased on going from control to 2,4-D treated sample, this result is consistent with [31], which can be explained as follows: the band at 2866cm^{-1} is generated just by symmetric stretching of CH_2 groups, whereas the 2921cm^{-1} band is attributed to contributions of asymmetric and symmetric motions of CH_2 and CH_3 groups respectively. In addition, the relative intensity of 2921cm^{-1} band can be influenced by methane C-H stretching absorption near 2900cm^{-1} [31], which results from oxidation of CH_2 groups to hydroxymethine groups. It is well known that CH_3 groups exhibit a minor susceptibility to oxidation than that of CH_2 groups, since the lipid acyl chains are oriented within the cell membrane so that the methyl groups are located in the hydrophobic interior.[22]. At the same time, the reduced νas(CH_2) / νs(CH_3) intensity ratio in 2,4-D treated brain tissue is also indication of higher lipid acyl chain unsaturation and polarity, which is known to occur with lipid acyl chain peroxidation.[32]

Cecilia *et al.,* [23] studied the perturbation of membrane dynamics in nerve cells during bilirubin-induced apoptosis by using spin labels and electron paramagnetic resonance spectroscopy analysis of whole cell and isolated mitochondrial membrane. Our results agree with their results and we can say assertively that, by physically interacting with cell membranes, 2,4-D induced decrease in lipid polarity sensed at a superficial level, increased the disorder and the looseness of lipid chain packing and increase the membrane fluidity. The enhanced membrane permeability coincided with an increase in lipid fluidity and protein mobility and was associated with significant oxidative injury to membrane lipids. [23] Tushcl & Schwab[33] studied the cytotoxic effects of the herbicide 2,4-D in hepatoma cell line HepG2. They suggested that the induction of apoptosis in HepG2 cells by 2,4-D was accompanied by disruption of the mitochondrial membrane potential as verified by staining with the cationic JC-1 probe. Moreover, upon 2,4-D toxicity, the formation of carbonyl compounds against lipase action or lipid degradation during lipid oxidation was significantly increased. As 2,4-D proved to induce apoptosis to nerve cells, apoptosis involves biochemical changes on DNA, protein and lipid, protein synthesis and/or the modification of existing proteins (such as caspases). Lipids are also heavily involved in apoptosis. DNA fragmentation, activation of caspases and externalization of phosphatidylserine are considered to be three biomarkers of apoptosis.[34] These results consistent with those found earlier, which suggest that the peaks at 1745(cholesterol and triglycerides ester C=O), 1720(carbonyl C-O stretch), and 1621cm-1(peptide C=O stretch) are positively correlated with LDL oxidation.[35]

These results strongly suggest that membrane phospholipids of brain tissue are attacked by free radical during oxidative stress mediated by 2,4-D treatment, which affect the lipid structure and lipid acyl chains saturation.[36] As 2,4-D is capable of binding itself with proteins, protein damage may be the result of direct impact of 2,4-D or its indirect effect, for example by generation of free radicals that results in protein peroxidation.[10]

The marked reduction observed in the area of amide B (around 3068cm^{-1}) band from 194.422 to 169.587 in the 2,4-D treated tissues together with the shift to lower frequency from 3068.848cm^{-1} to 3066.365 cm^{-1} upon 2,4-D treatment is an indicative to a decrease in protein content.[13] These results are consistent with the observed significant reduction in the intensity as well as area of amide I bands around 1654cm^{-1} in the brain spectrum due to 2,4-D intoxication which can be considered as a strong evidence of the decrease in the protein quantity of the system. This decrease is in agreement with the decreased observed in the Amide A/Amide B, Amide I /vas(CH2)lipids ratios together with the observed band shift of the amide B band which is shifted to lower values due to the toxic effect of 2,4-D. This could be a sign of the destructive effect of 2,4-D and could be attributed to a change in the composition of the whole protein pattern. [37] Cakmak et al., [38] have also observed decreasing intensity in amide A and amide I bands, trend in rainbow trout liver treated with 17β esradiol and nonylphenol. They elucidated this decreases in intensities of protein bands to alteration

of the protein synthesis and protein structure due to toxicities. Palaniappan and Vijayasundaram[13] also found a significant decrease in the intensity of amide A and amide I bands of the brain tissue of Labeo rohita due to arsenic intoxicatin, suggesting a decrease in protein quantity of rat brain tissue.

FTIR spectroscopy is one of the major techniques for the determination of protein secondary structures in various tissues. [39] After deconvolution and curve fitting to the amide I and amide II bands it was observed that the total area of α-helix secondary structure is decreased, while the total area of β-sheet structures increased due to the toxic effect of 2,4-D. The decrease in α-helix structure of the cerebellum brain tissues might be responsible for the increase in β-sheet structure, which was consistent with the mechanism of β-sheet formation. [13, 40] It is known that the β-sheet structure content in proteins can be formed by thermal- , salt-or solvent-induced aggregation [41] as a result of proteins denaturation. The β-sheet structure in 2,4-D intoxicated brain tissues suggests that the increase of the intermolecular hydrogen-bond interactions forms aggregates of higher molecular weight, and then modifies the secondary structure of proteins in brain tissues. [40] In apoptotic cells there is a significant intensity decrease in the region between 900-1300 cm^{-1}, which corresponds to the nucleic acid bands, with respect to viable cells. [42] This finding was consistent with our results since there is a marked reduction in this band area upon 2,4-D intoxication (data not shown). It is also agree with the results obtained by Liu and Mantsch [43] when they describe a new analytical method, based on infrared (IR) spectroscopy, to estimate the percentage of apoptotic leukemic cells in two different cell lines (CEM and K562), induced with etoposide (VP-16). They detected changes in protein secondary structure, the increase in the overall lipid content and the decrease in the amount of detectable DNA. The above mentioned results which characterize the IR spectral signatures, indicative of apoptosis, were also supported morphologically by the transmission electron microscope analysis.

Cerebellar granule cells showed that 2,4-D induced apoptosis to exposed cells.[44] Apoptotic cells were characterized by chromatin margination to nuclear membrane and shrinkage of cell cytoplasm which is consistent with Kaur *et al.*[27]. Apoptosis is a mechanism that is regulated by genes and includes engagement of some receptors such as Fas and TNF receptor 1, by their ligands, or by agents that disrupt the integrity of the cell. Some chemotherapeutic drugs, may also cause caspase-dependent as well as caspase-independent cell death mechanisms.[45]

The present results showed that the electron microscopic examination of 2,4-D treated rat brain revealed that mitochondria undergo various morphological changes such as swelling, loss of cristae and cytoplasm shrinkage and chromatin fragmentation signifying apoptotic changes as compared to control ones which exhibited normal and intact mitochondria which agree with Kaur *et al*.[27] who found that ultra structural changes shown by electron microscopy examination of rat brain following 2,4-D exposure provided a clear evidence that 2,4-D-induced morphological changes were consistent with apoptotic cell death.[27]

It has also been reported that 2,4-D induced neurotoxicity may be due to generation of free radicals.[30] When incubating rat cerebellar granule cells with 2,4-D *in vitro*, generation of reactive oxygen species (ROS) and activity of selenium-glutathione peroxidase (Se-GPx) are augmented.[37] Furthermore, chlorophenoxy acids structures are related to acetic acid and can form analogues of acetyl-CoA (e.g. 2,4-D-CoA) *in vitro*. Formations of such analogues can disrupt several pathways involving acetyl-CoA, including the synthesis of acetylcholine. Possible formation of choline esters may act as false cholinergic messengers.[46]

Oxidative damage occurs in mitochondria more than any other organelles in the cell because the existence of the respiratory chain in the mitochondria leads to the formation of damaging ROS. This oxidative damage may modify mitochondrial proteins, DNA and lipids which leads to mitochondrial bioenergetics failure leading to necrotic or apoptotic cell death.[47]

Further, it has been demonstrated that apoptosis and necrosis are connected with structural and functional alterations in mitochondrial membranes exposed to 2,4-D. Chlorophenoxy herbicides can also disrupt cell membrane transport mechanisms by competitively inhibiting and saturating the organic anion transport system in the choroid plexus, which facilitates the removal of toxic anions. [48]

Conclusion

To conclude, by using FTIR and EM morphologic analysis of cerebellum rat brain tissue exposed to 2,4-D, we detected major membrane perturbation. By physically interacting with cell membranes, 2,4-D induced an almost immediate decrease in lipid polarity sensed at a superficial level, increased the disorder and the looseness of lipid chain packing and increase the membrane fluidity. Moreover, a remarkable decrease in protein content and a change in secondary structure were evident. Thus, with addition to the morphological changes, all of which can be considered as apoptosis biomarkers. As apoptosis involves biochemical changes on DNA, protein and lipid in addition to membrane perturbation

features, FTIR spectroscopy proved to be able to observe changes in individual living cells resulting from various agents that may induce apoptosis.

Acknowledgments

Mr. Zaki Al-Asouli, Dr. Neamat Kotb, Dalal Albaroudi, Nourah Al-Otaibi, Rasha Ahmed, Rula Habbal, Mr. Mohammad Refai and Amal Al- Mustadi.

This research work was supported by King Abdulaziz City for Science and Technology; grant number: AT-125-18

Corresponding authors
Gehan A. Raouf
Medical Biophysics Lab., King Fahd Medical Research Centre; Biochemistry Dept., King Abdulaziz University, 21551 Jeddah –KSA B.O.Box:42805, Spectroscopy Dep. Physics Div.-National Research, Cairo- Egypt.
gehan_raouf@hotmail.com - jahmed@kau.edu.sa

References

1. Raseir, G., J. Toppari, P. A.S., and J. B. Bourguignor., 2006. Female sexual maturation and reproduction after prepubertal exposure to estrogens and endocrine disrupting chemicals: A review of rodent and human data. *Mol. Cell Endocrinol*. **254-255**: 187–201.
2. Garabrant D.H., and M.A. Philbert. 2002. Review of 2,4-dichlorophenoxyacetic acid (2,4-D) epidemiology and toxicology. *Crit. Rev. Toxicol.* , **32**: 233.
3. Brand R.M., M. Spalding, and C. Mueller. , 2002. Sunscreens Can Increase Dermal Penetration of 2,4-Dichlorophenoxyacetic Acid. *Clin. Toxicol.* , **40**: 827.
4. Bortolozzi, A., A. M. Evangelista de Duffard, F. Daja, R. Duffard, and R. Silveira. 2001. Intracerebral administration of 2,4-dichlorophenoxyacetic acid induces behavioral and neurochemical alterations in the rat brain. *Neurotoxicology*. **22**: 221–232.
5. Tayeb, W., A. Nakbi, M. Trabelsi, N. Attia, A. Miled, and M. Hammamia. , 2010. Hepatotoxicity induced by sub-acute exposure of rats to 2,4-dichlorophenoxyacetic acid based herbicid "désormone lourd". *Journal of Hazardous Materials*. **180**: 225-33.
6. Lee, K., V. L. Johnson, and B. R. Blakley. 2001. The effect of exposure to a commercial 2,4-d formulation during gestation on the immune response in cd-1 mice. *Toxicology*. **165**: 39–49.
7. Morgan, M. K., P. R. Scheuerman, C. S. Bishop, and R. A. Pyles. , 1996. Teratogenic potential of atrazine and 2,4-d using fetax. *Journal of Toxicology and Environmental Health*. **48**: 58–61.
8. Garry, V. F., R. E. Tarone, I. R. Kirsch, J. M. Abdallah, D. P. Lombardi, L. K. Long, B. L. Burroughs, D. B. Barr, and J. S. Kesner. , 2001. Biomarker correlations of urinary 2,4-d levels in forester: Genomic instability and endocrine disruption. *Environmental Health Perspectives*. **109**: 495–500.
9. Gomez, L., F. Soler, S. Martinez, A. Gazquez, E. Duran, and V. Roncero. , 1999. 2,4-d treatment in tench (tinca tinca l.): Pathological processes on the excretory kidney. *Bulletin of Environmental Contaminants and Toxicology*. **62**: 600–607.
10. Bukowska, B. 2006. Toxicity of 2,4-dichlorophenoxyacetic acid – molecular mechanisms. *Polish J. of Environ. Stud.,* **15**: 365-374.
11. Raouf, G. A., A. Al-Malki, N. Mansouri, and R. Mahmoudi. , 2011. Preliminary study in diagnosis and early prediction of preeclampsia by using FTIR spectroscopy technique. *Life Science Journal*. **8**: 827-836.
12. Akkas, S. B., M. Severcan,, O. Yilmaz, and F. Severcan., 2007. Effects of lipoic acid supplementation on rat brain tissue: An ftir spectroscopic and neural network study. *Food Chemistry*, **105**: 1281–1288.
13. Palaniappan, P., and V. Vijayasundaram. 2009. The FTIR study of the brain tissue of labeo rohita due to arsenic intoxication. *Microchemical J.* . **91**: 118-124.
14. Sasic, S., M. Morimoto, M. Otsuka, and Y. Ozaki. , 2005. Two—dimensional correlation spectroscopy as a tool for analyzing vibrational images. *Vibr. Spec.* **37**: 217–24.
15. D'Souza, L., P. Devi, M.P. Shridhar, and G. Naik. , 2008. Use of Fourier Transform Infrared (FTIR) Spectroscopy to Study Cadmium-Induced Changes in Padina Tetrastromatica. *Analytical Chemistry Insights*. **3**: 135–143.
16. Severcan F., G. Gorgulu, G. T.S., and G. T. , 2005. Rapid monitoring of diabetes-induced lipid peroxidation by fourier transform infrared spectroscopy: Evidence from rat liver microsomal membranes. *Anal. Biochem.* , **339**: 36-40.
17. Carmona, P., A. Rodrý´guez-Casado, I. Alvarez, I. de Miguel, and A. Toledano. 2008. Ftir microspectroscopic analysis of the effects of certain drugs on oxidative stress and brain protein structure,. *Biopolymers*. **89**: 548-554.
18. Crupi, V., D. Majolino, P. Migliardo, M. R. Mondello, M. P. German, and S. Pergolizzi. , 2001. Ft-ir molecular evidence of liver damage by chemical agents. *Vibrational Spectroscopy*. **25**: 213-222.
19. Borchman, D., F. Giblin, V. Leverenz, V. Reddy, Lin Li-Ren, M. Yappert, D. Tang, and L. Li. , 2000. Impact of aging and hyperbaric oxygen *in vivo* on guinea pig lens lipids and nuclear light scatter. *Invest Ophthalmol Vis Sci.* , **41**: 3061–3073.
20. Van de Voort, F. R., A. A. Ismail, J. Sedman, and G. Emo. , 1994. Monitoring the oxidation of edible oils by fourier transform infrared spectroscopy. *J Am Oil Chem Soc.* , **71**: 243–253.
21. Fraile M. V., B. Patrón-Gallardo, G. López-Rodríguez, and C. P. , 1999. Ftir study of multilamellar lipid dispersions containing cholesteryl linoleate and dipalmitoylphosphatidylcholine. *Chem. Phys. Lipids*. **97**: 119-128.
22. Rodriguez-Casado J., M. I. Alvarez, E. De Miguel, T. A., and P. Carmona. , 2007. Amphetamine effects on oxidative stress and formation of proteic beta-sheet structures as revealed by ftir microspectroscopy. *Biopolymers*. **86**: 437-446.

23. Cecília, M. P., S. Susana, E. Rui, A. Pedro, B. Dora, J. José, and G. Moura. , 2002. Perturbation of membrane dynamics in nerve cells as an early event during bilirubin-induced apoptosis. *Journal of Lipid Research*. **43**: 885-894.
24. Diem, M., S. Boydston-White, and L. Chiriboga. , 1999. Infrared spectroscopy of cells and tissues. Shining light onto an unsettled subject. *Appl. Spectrosc*. **53**: 148A–161A.
25. Takahashi, H., S. W. French, and P. T. T. Wong. , 1991. Alterations in hepatic lipids and proteins by chronic ethanol intake: A high pressure fourier transform infrared spectroscopic study on alcoholic liver disease in the rat. *Alcoholism-Clinical and Experimental Research*. **15**: 219–223.
26. Binukumar, B. K., B. Amanjit, K. Ramesh, and D. G. Kiran., 2010. Nigrostriatal neuronal death following chronic dichlorvos exposure: crosstalk between mitochondrial impairments, a synuclein aggregation, oxidative damage and behavioral changes. *Molecular Brain*. **3**: 35-55.
27. Kaur, P., B. Radotra, R. W. Minz, and K. D. Gill., 2007. Impaired mitochondrial energy metabolism and neuronal apoptotic cell death after chronic dichlorvos (OP) exposure in rat brain. *Neurotoxicology*. **28**: 1208-1219.
28. Sharma, Y., S. Bashir, M. Irshad b, T. C. Nagc, and T. D. Dogra. , 2005. Dimethoate-induced effects on antioxidant status of liver and brain of rats following subchronic exposure. *Toxicology*. **215**: 173–181.
29. Mates, J. M. , 2000. Effects of antioxidant enzymes in the molecular control of reactive oxygen species toxicology. *Toxicology*. **153**: 83-104.
30. Bukowska, B., B. Rychlik, A. Krokosz, and J. Michalowicz. , 2008. Phenoxyherbicides induce production of free radicals in human erythrocytes: Oxidation of dichlorofluorescine and dihydrorhodamine by 2,4-d-na and mcpa-na. *Food Chem. Toxicol.* **46**: 359-367.
31. Socrates, G. 2001. Infrared and Raman characteristic groups frequencies. Tables and charts, Chichester: Wiley press.
32. Petibois, C., G. Cazorla, J. R. Poortmans, and G. Déléris. , 2003. Biochemical aspects of overtraining in endurance sports: The metabolism alteration process syndrome. *Sports Medicine*. **33**: 83-94.
33. Tuschl, H. and C. Schwab. ,2003. Cytotoxic effect of the herbicide 2,4-dichlorophenoxyacetic acid in hepg2 cells. *Food and Chemical Toxicilogy*, **41**: 385-393.
34. Thompson, C. B. 1995. Apoptosis in the pathogenesis and treatment of disease. *Science*. **267**: 1456-1462.
35. Mantsch, H. H. , 2001. Apoptosis-induced structural changes in leukemia cells identified by ir spectroscopy. *J. Mol. Str*. **565-566**: 299-304.
36. Inouyea, M., T. Miob, and K. Suminob. , 1999. Formation of 9-hydroxy linoleic acid as a product of phospholipid peroxidation in diabetic erythrocyte membranes. *Biochem. Biophys. Acta*. **1438**: 204-212.
37. Bongiovanni, B., P. De Lorenzi, A. Ferri, C. Konjuh, M. Rassetto, A. M. Evangelista de Duffard, D. P. Cardinali, and R. Duffard. , 2007. Melatonin decreases the oxidative stress produced by 2,4-dichlorophenoxyacetic acid in rat cerebellar granule cells. *Neurotox Res*. **11**: 93-99.
38. Cakmak G., T. I., and F. Severcan. , 2006. 17b-estradiol induced compositional, structural and functional changes on rainbow trout liver, revealed by ftir spectroscopy: A comparative study with nonylphenol. *Aquatic Toxicology*. **77**: 53-63.
39. Severcan, F., and P. Haris. , 2003. The main unfolding and aggregation of pcs is preceded by the unfolding of a minor structure at lower temperature. *Biopolymers*. **69**: 440-447.
40. Creighton, T. , 1984. Pathways and mechanisms of protein folding. *Adv. Biophys*. 18: 1-20.
41. Kim, Y., C. A. Rose, Y. Liu, Y. Ozaki, G. Datta, and A. T. Ut. ,1994. Ft-ir and near-infrared ft-raman studies of the secondary structure of insulinotropin in the solid state: Á-helix to â-sheet conversion by phenol and/or high shear force. *J Pharm Sci.* **83**: 1175–1180.
42. Fabio, G., and M. Marta. ,2003. Monitoring of apoptosis of HL60 cells by Fourier-transform infrared spectroscopy. *Biochem. J.* **369**: 239–248.
43. Liu, K. Z., and H. H. Mantsch. , 2001. Apoptosis-induced structural changes in leukaemia cells identified by IR spectroscopy. *J Mol Struct.* **565-566**: 299-344.
44. De Moliner, K. L., A. M. Evangelista de Duffard, E. Soto, R. Duffard, and A. M. Adamo. , 2002. Induction of Apoptosis in Cerebellar Granule Cells by 2,4-Dichlorophenoxyacetic Acid. *Neurochemical Research*. **27**: 1439-1446.
45. Glaser, T., B. Wagenknecht, P. Groscurth, P. H. Krammer, and M. Weller. , 1999. Death ligand/receptor-independent caspase activation mediates drug-induced cytotoxic cell death in human malignant glioma cells. *Oncogene*. **18**: 5044-5053.
46. Bradberry S.M., B.E. Watt, A.T. Proudfoot. and J.A. Vale. , 2000. Mechanism of toxicity, clinical features and management of acute chlorophenoxy herbicide poisoning: a review. *Clin. Toxicology*. **38**: 111-122.
47. Smith, R. A. J., C. M. Porteous, and C. M. Murphy. , 1999. Selective targeting of an antioxidant to mitochondria. *Eur J Biochem*. **263**: 709–16.
48. Kim, C. S., and J. B. Pritchard. 1993. Transport of 2,4,5-trichlorophenoxyacetic acid across the blood-cerebrospinal fluid barrier of the rabbit. *J. Pharmacol. Exp. Ther.* **267**: 751–757.

10/5/2012